Isotropic-to-nematic transition in liquid-crystalline heteropolymers: II. Side-chain liquid-crystalline polymers

2006 J. Phys.: Condens. Matter 18 9359

(http://iopscience.iop.org/0953-8984/18/41/004)

INSTITUTE OF PHYSICS PUBLISHING JOURNAL OF PHYSICS: CONDENSED MATTER

J. Phys.: Condens. Matter **18** (2006) 9359–9374 doi:10.1088/0953-8984/18/41/004

Isotropic-to-nematic transition in liquid-crystalline heteropolymers: II. Side-chain liquid-crystalline polymers

Paul P F Wessels[1] **and Bela M Mulder**

FOM Institute for Atomic and Molecular Physics (AMOLF), Kruislaan 407, 1098 SJ Amsterdam, The Netherlands

E-mail: mulder@amolf.nl

Received 19 January 2006, in final form 28 June 2006
Published 29 September 2006
Online at stacks.iop.org/JPhysCM/18/9359

Abstract

We apply a density functional approach for arbitrary branched liquid-crystalline (LC) heteropolymers consisting of elongated rigid rods coupled through elastic joints developed in a companion paper (Wessels and Mulder 2006 *J. Phys. Condens. Matter.* **18** 9335) to a model for side-chain liquid-crystalline polymers. In this model mesogenic units are coupled through finite-length spacers to a linear backbone polymer. The stereochemical constraints imposed at the connection between spacer and backbone are explicitly modelled. Using a bifurcation analysis, analytical results are obtained for the spinodal density of the I–N transition and the variation of the degree of ordering over the various molecular parts at the instability as a function of the model parameters. We also determine the location of the crossover between oblate and prolate backbone conformations in the nematic phase.

1. Introduction

Liquid-crystalline (LC) polymers combine the the optical properties of liquid crystals with the mechanical and processing characteristics of polymers. To create such LC polymers low-molecular-weight liquid-crystal forming moieties, called mesogens, are either directly incorporated into a linear polymer backbone (main-chain LC polymers) or laterally attached to them (side-chain LC polymers). To achieve an optimal balance of properties, it is essential that, on the one hand, the mesogens can freely interact to drive orientational ordering, while on the other hand the polymer backbone retains a sufficient amount of conformational entropy. Apart from the technological interest in the combination of properties mentioned above, these conflicting tendencies give rise to a rich phase behaviour and these systems are therefore also interesting from a fundamental perspective [1–6]. The practical solution for achieving

[1] Present address: ABN-AMRO Corporate Research, Amsterdam, The Netherlands.

0953-8984/06/419359+16$30.00

the necessary balance of tendencies has turned out to be the insertion of more flexible moieties within the polymers in the form of aliphatic spacer chains [7–9]. These spacers effectively spatially decouple the mesogens, minimizing any stereo-chemical frustration to the LC ordering process, while the polymer chain as a whole can still have an approximately coil-like conformation.

In the companion paper [10], hereafter referred to as I, we have set up a general formalism for describing the phase behaviour of arbitrary branched liquid-crystalline (LC) heteropolymers consisting of elongated rigid rods coupled through elastic joints. Here we will apply this formalism to model side-chain polymers.

The history of understanding of the molecular origin of LC order has a few definite milestones. The seminal paper of Onsager on the explanation of nematic LC order in colloidal suspensions of rigid hard rodlike particles [11], which introduced the concept of excluded volume, focused on entropic effects. The mean field theory of Maier and Saupe [12] successfully made contact with the large number of data on thermotropic liquid crystals. The role of molecular flexibility was first discussed by Khokhlov and Semenov (KS) [13, 14] by extending Onsager's theory to hard wormlike chains, and later by Warner and co-workers [15], who similarly extended the Maier–Saupe theory. We refer the reader to I for a review of how these elements can be combined to make models of main-chain LC polymers.

Given the additional complexity, due to their heterogeneous composition and branched geometry, it is not surprising that much less work has been done on LC ordering in side-chain LC polymers. Khokhlov and co-workers first used a Flory type lattice approach [16, 17]. Later on a more realistic off-lattice model for side-chain LC polymers was considered by Warner *et al* (WWR) [18, 19]. In their model rigid mesogenic side-groups are directly laterally connected to a semi-flexible backbone. Except for the bending interactions of the wormlike backbone, all interactions between the various molecular components are treated in a Maier–Saupe type mean-field manner. They have explored the full (nematic) phase diagram, finding three nematic phases, first-order phase transition between them and a critical point. Later on, they included biaxial phases as well [20]. However, their model does not take into account that in reality additional spacers are used as lateral connectors between the mesogens and the backbone. Moreover, the stereo-chemical constraints on the relative orientation of the side-groups with respect to the backbone are also treated as a mean-field cross-interaction, and therefore not on the same footing as the bending interactions of the backbone, this in spite of the fact that all these interactions, which are related to the way the various molecular components are linked together to form the whole polymer, are similar in origin and as short-range intra-molecular interactions distinct from the inter-molecular orientational interactions. One aim of the present work is to specifically address these two shortcomings.

The generic model for side-chain LC polymers we consider in this paper consist of three different components: a polymer backbone, mesogens and spacer chains, that laterally connect these mesogens to the backbone. All these components are modelled as consisting of hard, slender, cylindrically symmetric rods connected through appropriate bending potentials. The formalism we have developed in I allows us to deal with the intra-molecular interactions of such a branched, but simply connected, molecule exactly. The inter-molecular interactions are treated within the Onsager approximation. Both for the backbone polymer and the lateral spacer chains we take the wormlike chain limit. Moreover, we let the number of polymer repeat units go to infinity, disregarding any end effects. The remaining theory is fully described by six parameters: the length, the persistence length and the diameters of both the backbone, within a single repeat unit, and the lateral spacers, all measured in units relative to the mesogen length and diameter respectively. A brief report, containing a number of numerical results on this model, has been presented elsewhere [21].

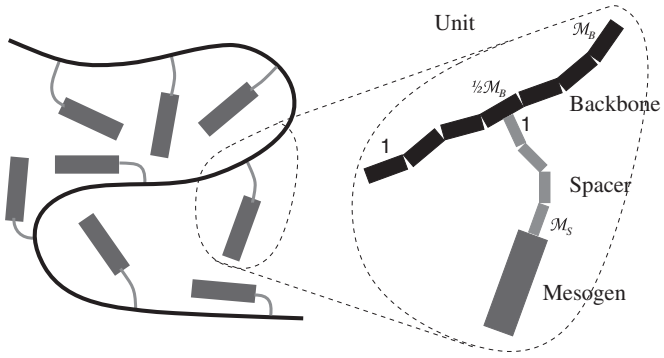

Figure 1. The model of a side-chain LC polymer we employ, with the inset showing the labelling of the segments in the different components.

The outline of the paper is as follows. In section 2.1 we briefly recall the formalism presented in more detail in I, setting up the free-energy functional, discussing the appropriate stationarity equations, discussing the isotropic–nematic phase equilibrium and formulating the wormlike-chain limit, which is applied to both the backbone and the spacer chains. In section 3 we turn to the results, first performing a bifurcation analysis of the isotropic phase. This yields an analytical determination of the isotropic–nematic spinodal. We explicitly determine the values of the model parameters for which the backbone conformation crosses over from prolate to oblate with respect to the preferred orientation of the mesogens. Finally, we present the relative degree of order along a polymer repeat unit and compare with some numerical results presented earlier for the same model [21].

2. Formalism

2.1. Model

We consider a fluid N LC polymers in a volume V, where we denote the polymer number density as $\rho = N/V$. The polymers consist of a *backbone* (denoted by B) with side-chains attached laterally at regular distances. Each side-chain consists of a rigid *mesogen* (M) connected to the backbone via a flexible *spacer* (S). A repeating section of the backbone with a single side-chain attached we refer to as a *unit*, and there are $\mathcal{N}$ of these units in the polymer (see figure 1). The polymer is modelled as a segmented chain, with the segments being slender cylindrical rods. Within a unit, each of the three different components τ, where $\tau \in \{\mathrm{B}, \mathrm{S}, \mathrm{M}\}$, consists of $\mathcal{M}_\tau$ segments characterized by a length l_τ and a width d_τ with $l_\tau \gg d_\tau$. Consequently, there are $\mathcal{N}\mathcal{M}_\tau$ segments of each component in the whole chain and by definition there is only one mesogen per unit, hence $\mathcal{M}_\mathrm{M} = 1$. Every segment has a label m which specifies its location in the chain but is also assumed to (implicitly) contain its type-specification, i.e. by the notation $m \in \tau$ we mean that segment m is a type-τ segment. Additionally, each segment has an orientation $\hat{\omega}_m$, which is a unit vector pointing along the long axis of the segment. The conformation of the whole polymer is then given by the orientations of all segments $\mathbf{\Omega} = \{\hat{\omega}_1, \hat{\omega}_2, \ldots, \hat{\omega}_{\mathcal{N}(\mathcal{M}_\mathrm{B}+\mathcal{M}_{\mathrm{S}+1})}\}$.

We assume a bending potential $u_{m,m'} = u_{\tau,\tau'}$ between any two segments $m \in \tau$ and $m' \in \tau'$ which are nearest neighbours in the polymer,

$$
\begin{aligned}
u_{\mathrm{B,B}}(\hat{\omega}_m, \hat{\omega}'_{m'}) &= -J_{\mathrm{B}}\hat{\omega}_m \cdot \hat{\omega}'_{m'} \\
u_{\mathrm{B,S}}(\hat{\omega}_m, \hat{\omega}'_{m'}) &= \begin{cases} 0 & \text{if } \hat{\omega}_m \cdot \hat{\omega}'_{m'} = 0 \\ \infty & \text{if } \hat{\omega}_m \cdot \hat{\omega}'_{m'} \neq 0 \end{cases} \\
u_{\mathrm{S,S}}(\hat{\omega}_m, \hat{\omega}'_{m'}) &= -J_{\mathrm{S}}\hat{\omega} \cdot \hat{\omega}'_{m'} \\
u_{\mathrm{S,M}}(\hat{\omega}_m, \hat{\omega}'_{m'}) &= -J_{\mathrm{S}}\hat{\omega} \cdot \hat{\omega}'_{m'}
\end{aligned}
\tag{1}
$$

which is obviously symmetric, $u_{\tau,\tau'} = u_{\tau',\tau}$. The BB, SS and SM potentials favour mutual alignment and oppose bending in a generic fashion via the orientational coupling constants J_{B} and J_{S} for the backbone and the spacer respectively. The BS potential uniquely selects a perpendicular arrangement, in order to force (at least locally) the spacers to be at right angles with the backbone, which mimics the stereo-chemical constraints inherent in this attachment. Concerning the interaction between different polymers, we assume only hard-body repulsion between the segments, meaning that the potential is infinity when two segments overlap and zero when they do not [11].

2.2. *Stationarity equations*

Within density functional theory the free energy is a functional of the single-molecule configuration distribution function [22]. In the present case, we only consider homogeneous fluid phases, so this function has no spatial dependence and it reduces to $\rho f(\mathbf{\Omega})$. We call the function $f(\mathbf{\Omega})$ the *conformational distribution function* (CDF), which is normalized as follows $\int \mathrm{d}\mathbf{\Omega}\, f(\mathbf{\Omega}) = 1$ where $\int \mathrm{d}\mathbf{\Omega} = \int \prod_k \mathrm{d}\hat{\omega}_k$. The density functional (in terms of $f(\mathbf{\Omega})$) for our system in the second virial (or Onsager) approximation is given by

$$
\begin{aligned}
\frac{\beta\mathcal{F}[f]}{N} &= \log(\rho\mathcal{V}_{\mathrm{T}}) + \int \mathrm{d}\mathbf{\Omega}\, f(\mathbf{\Omega})\left[\log f(\mathbf{\Omega}) - 1\right] \\
&\quad + \beta\int \mathrm{d}\mathbf{\Omega}\, f(\mathbf{\Omega})U(\mathbf{\Omega}) + \tfrac{1}{2}\rho\int \mathrm{d}\mathbf{\Omega}\,\mathrm{d}\mathbf{\Omega}'\, f(\mathbf{\Omega})f(\mathbf{\Omega}')\mathcal{E}(\mathbf{\Omega},\mathbf{\Omega}').
\end{aligned}
\tag{2}
$$

Here, $\beta = 1/k_{\mathrm{B}}T$, k_{B} the Boltzmann constant, T the temperature and $\mathcal{V}_{\mathrm{T}}$ is a product of the relevant de Broglie thermal wavelengths. The quantity $U(\mathbf{\Omega})$ is the total internal energy of the polymer and is given by

$$
U(\mathbf{\Omega}) = \sum_{m,m'}^{(m,m')} u_{m,m'}(\hat{\omega}_m, \hat{\omega}_{m'}),
\tag{3}
$$

where the sum runs over all m and m' which are nearest neighbours in the chain (notation: (m, m'), note that m and m' do not need to be of the same type). In fluid phases of hard-body molecules a central role is played by the so-called excluded volume $\mathcal{E}(\mathbf{\Omega}, \mathbf{\Omega}')$ between two molecules. It is approximated as the sum over all segment–segment excluded volumes,

$$
\mathcal{E}(\mathbf{\Omega}, \mathbf{\Omega}') = \sum_{m,m'} e_{m,m'}(\hat{\omega}_m, \hat{\omega}'_{m'}).
\tag{4}
$$

which are $e_{m,m'} = e_{\tau,\tau'}$ for $m \in \tau$ and $m' \in \tau'$. For very slender rods ($l_\tau \gg d_\tau$) these are given by

$$
e_{\tau,\tau'}(\hat{\omega}_m, \hat{\omega}'_{m'}) = l_\tau l_{\tau'}(d_\tau + d_{\tau'})|\sin\gamma(\hat{\omega}_m, \hat{\omega}'_{m'})|,
\tag{5}
$$

where $\gamma(\hat{\omega}, \hat{\omega}')$ is the planar angle between $\hat{\omega}$ and $\hat{\omega}'$.

At this point, we note that three approximations have been made; we neglect

(i) interactions between three or more chains simultaneously (Onsager approximation),

(ii) simultaneous interactions between two chains involving more than one pair of segments (equation (4)) and
(iii) overlaps of segments on the same chain (equation (3)).

For homogeneous bulk phases these approximations are commonly assumed to be reasonable and to retain the essential physics [23, 24]. Furthermore, we stress that for sufficiently slender segments ($l_\tau \gg d_\tau$) the Onsager description becomes exact [11, 25].

In equilibrium, the free energy reaches a minimum and the functional is stationary, i.e. $\delta\mathcal{F}/\delta f(\mathbf{\Omega}) = N\mu$, where μ is the chemical potential acting as a Lagrange multiplier enforcing the normalization of $f(\mathbf{\Omega})$. This yields the following Euler–Lagrange equation:

$$\log f(\mathbf{\Omega}) + \beta U(\mathbf{\Omega}) + \rho \int \mathrm{d}\mathbf{\Omega}' f(\mathbf{\Omega}')\mathcal{E}(\mathbf{\Omega}, \mathbf{\Omega}') = \beta\mu, \tag{6}$$

where μ can be eliminated using $\int \mathrm{d}\mathbf{\Omega}\, f(\mathbf{\Omega}) = 1$.

Via the following projection, we define the single-segment *orientational distribution function* (ODF),

$$f_m(\hat{\omega}_m) = \int \prod_{k\neq m} \mathrm{d}\hat{\omega}_k\, f(\mathbf{\Omega}), \tag{7}$$

where the integration is over all $\hat{\omega}_k$ except the mth. Inserting the detailed forms (equations (1), (3), (4) and (5)) in equation (6) and using equation (7), we obtain the following set of coupled equations in terms of the ODFs:

$$f_m(\hat{\omega}_m) = Q^{-1} \int \prod_{k\neq m} \mathrm{d}\hat{\omega}_k \prod_{k,k'}^{(k,k')} w_{k,k'}(\hat{\omega}_k, \hat{\omega}_{k'}) \prod_k \exp\left[-\rho \sum_{k'} \int \mathrm{d}\hat{\omega}' e_{k,k'}(\hat{\omega}_k, \hat{\omega}') f_{k'}(\hat{\omega}')\right]. \tag{8}$$

In order to ease notation we have introduced $w_{k,k'}(\hat{\omega}_k, \hat{\omega}_{k'}) = \exp[-\beta_\mathrm{B} u_{k,k'}(\hat{\omega}_k, \hat{\omega}_{k'})]$. A more detailed version of the derivation of equation (8) is given in [25] for linear homopolymers and [10] for general heteropolymers.

2.3. Isotropic and nematic phases

The isotropic phase, in which $f_m(\hat{\omega}_m) = 1/4\pi$, is always a solution to equations (8), and at low densities also (globally) stable. At higher densities the mesogen–mesogen interactions will drive the system towards an orientationally ordered phase: the nematic. Here we only consider uniaxial nematics and consequently it suffices to use the standard Maier–Saupe order parameter as a measure of the orientational order of a segment m,

$$S_m = 2\pi \int_0^\pi \mathrm{d}\theta \sin\theta\, P_2(\cos\theta)\, f_m(\theta), \tag{9}$$

with the factor 2π in front due to the azimuthal integration ($\int \mathrm{d}\hat{\omega} = \int_0^\pi \mathrm{d}\theta \sin\theta \int_0^{2\pi} \mathrm{d}\phi$). The average degree of order per component can be defined straightforwardly: $S_\tau = 1/M_\tau \sum_{m\in\tau} S_m$. In the isotropic phase, $S_\tau = 0$ for all three components $\tau \in \{\mathrm{B}, \mathrm{S}, \mathrm{M}\}$. In the nematic phase, the mesogens order with respect to a certain preferred direction, given by the director $\hat{n}$, and, because of their direct connection to the mesogens, the same will happen to the spacers, $0 < S_\mathrm{M}, S_\mathrm{S} < 1$. However, the backbone experiences two mutually opposing contributions: (i) via the spacers a tendency to orient perpendicular to the mesogens is transferred whereas (ii) due to the external (nematic) field a parallel arrangement is favoured. If the first effect dominates the net nematic order is negative $S_\mathrm{B} < 0$ and the backbone will be in an oblate conformation, whereas if the second effect wins the backbone will have a

positive order $S_B > 0$ and be in prolate conformation[2]. If the spacers are relatively short and therefore stiff, the result will be an 'oblate nematic' (ON), and if they are longer and floppier a 'prolate nematic' (PN) results. The excluded volume term in the free energy scales with density, whereas intrachain bending (elastic) energy does not depend on density. Therefore, for higher densities the system will eventually always favour a PN phase. Upon compression we thus expect to find a phase sequence I–ON–PN or directly I–PN. In [10], we have studied numerical solutions to equations (8) for this system, locating the I–N coexistence and computing the dependence of the order parameters of the various components in the nematic phase. It can be shown that the transition from ON to PN is continuous and is in fact not a thermodynamic phase transition [21, 10]. In this paper, we restrict ourselves to the I–N transition and study the properties of the I–N bifurcation point. Furthermore, we compare some of the bifurcation results on the I–N transition to the numerical results of [21].

2.4. Wormlike chains and infinite backbones

Since Khokhlov and Semenov [13, 14], the wormlike chain concept is widely used to model nematic ordering in partially flexible molecules. Wormlike chains are continuously flexible objects characterized by a persistence length [26]. In order to reduce the number of model parameters we transform our segmented backbone and lateral spacers in wormlike chains by applying the so-called wormlike chain limit (WCL). Going from our system of segmented chains to continuously flexible chains, the WCL can be formulated as [25]

$$\begin{aligned} l_B &\to 0, \qquad \beta J_B \to \infty, \qquad \mathcal{M}_B \to \infty \\ l_S &\to 0, \qquad \beta J_S \to \infty, \qquad \mathcal{M}_S \to \infty \end{aligned} \tag{10}$$

where the following products and ratios stay finite:

$$\begin{aligned} P_B &= \beta J_B l_B \qquad \bar{\mathcal{M}}_B = \mathcal{M}_B/\beta J_B \\ P_S &= \beta J_S l_S \qquad \bar{\mathcal{M}}_S = \mathcal{M}_S/\beta J_S, \end{aligned} \tag{11}$$

where the quantities P_B and P_S turn out to be the persistence lengths and $\bar{\mathcal{M}}_B$ and $\bar{\mathcal{M}}_S$ the number of persistence lengths in one repeat unit [25]. Throughout this paper, an overbar denotes quantities obtained after taking the WCL. By applying the WCL to the backbone and the spacers we can drop two model parameters: $l_B, J_B, \mathcal{M}_B \to P_B, \bar{\mathcal{M}}_B$ and $l_S, J_S, \mathcal{M}_S \to P_S, \bar{\mathcal{M}}_S$.

We can proceed simplifying the system and drop another model parameter by assuming that the backbone is infinitely long. In this way, every unit is effectively located in the 'middle' of the polymer, since the influence of the free ends of the backbone is zero. We call this the infinite backbone limit (IBL),

$$\mathcal{N} \to \infty \qquad \rho \to 0 \qquad \text{with } \eta = \rho\mathcal{N} \text{ finite}, \tag{12}$$

where the polymer density ρ has to go to zero in order to obtain a finite unit density η (= mesogen density, which is driving the LC phase transitions). This limit allows us to consider (effectively) only a single unit, as every unit in the chain is exactly the same as its neighbour, and as a consequence there are no 'free end effects'.

Finally, as our system is scale invariant we can use dimensionless length scales. The mesogens are the largest segments (they are the liquid-crystal formers) and are not subject to the WCL, and therefore we choose to measure all other lengths in units of l_M and d_M, i.e. $\tilde{P}_\tau = P_\tau/l_M$ and $\tilde{d}_\tau = d_\tau/d_M$ with $\tau \in \{B, S\}$, with the tilde denoting dimensionless

[2] Strictly speaking the connection between the positive sign of the nematic order of the backbone $S_B > 0$ ($S_B < 0$) and prolate (oblate) conformations (which are determined by the radii of gyration of the backbone parallel and perpendicular to the nematic field) is not trivial. There is, however, a rough correspondence and we will proceed bearing this in mind.

quantities. As a result this reduces the set of effective model parameters to six, i.e. $\tilde{P}_B$, $\tilde{d}_B$ and $\bar{\mathcal{M}}_B$ for the backbone, and $\tilde{P}_S$, $\tilde{d}_S$ and $\bar{\mathcal{M}}_S$ for the spacers (the mesogens now have unit dimensions for both the length and the width). The only thermodynamic intensive variable is the unit density, η, which can be made dimensionless with the prefactor of the MM excluded volume: $\tilde{\eta} = 2\rho\mathcal{N}l_M^2 d_M$. A special case we find instructive, and frequently use, is obtained by setting $\tilde{d}_B = \tilde{d}_S = 0$ and $\tilde{P}_B = \tilde{P}_S$, leaving only three model parameters. In this case, the backbone and spacers have zero thickness, and the BB, BS and SS excluded volumes are zero, but the BM, SM and of course the MM interactions are not. In spite of the above limits and simplifications, we believe the essential physics is still retained.

3. Bifurcation analysis

3.1. Bifurcation density

The stationarity equations can be studied by means of an I–N bifurcation analysis to locate the density where the nematic solution branches off the isotropic. Thereto, we substitute isotropic distributions with infinitesimal (ε) nematic perturbations, $f_m(\hat{\omega}_m) = 1/4\pi + \varepsilon c_m P_2(\hat{\omega}_m \cdot \hat{n})$ in the stationarity equations, equations (8). Subsequent linearization with respect to ε, performance of the integrals and averaging over all segments belonging to the same type yields the following three-dimensional matrix eigenvalue equation:

$$\mathbf{c} = -\frac{\rho}{4\pi}\mathbf{W}^{(2)}\mathbf{E}^{(2)}\mathbf{c}. \tag{13}$$

The details of this derivation are given in I. In this equation the lowest (positive) solution for the density ρ is identified as the 'physical' bifurcation density ρ_*. The corresponding solution for the components of $\mathbf{c}$ represents the average relative degree of ordering of each of the types of components at the bifurcation, $c_{\tau,*} = \frac{1}{M_\tau}\sum_{k\in\tau} c_{k,*}$ (which we will normalize by setting the mesogen order to one, $c_{M,*} = 1$). The matrices $\mathbf{W}^{(2)}$ and $\mathbf{E}^{(2)}$ depend on molecular parameters and correspond to intramolecular (due to flexibility) and intermolecular (due to excluded volume) interaction contributions respectively. The definitions of $\mathbf{W}^{(2)}$ and $\mathbf{E}^{(2)}$, in terms of segmented chains, are given below, after which they are evaluated in the WCL and the IBL.

We consider first the excluded volume matrix, which is defined as [10]

$$E^{(2)}_{\tau,\tau'} = \mathcal{N}^2\mathcal{M}_\tau\mathcal{M}_{\tau'}e^{(2)}_{\tau,\tau'} = s_2\mathcal{N}^2\mathcal{M}_\tau l_\tau\mathcal{M}_{\tau'}l_{\tau'}(d_\tau + d_{\tau'}), \tag{14}$$

where $e^{(2)}_{\tau,\tau'}$ and $s_2 = -\pi^2/8$ are the second order Legendre coefficients of $e_{\tau,\tau'}(\hat{\omega}\cdot\hat{\omega}')$ (from equation (5)) and $|\sin\gamma(\hat{\omega}\cdot\hat{\omega}')|$ respectively. We choose to order the types in the sequence B, S, M. We normalize $\mathbf{E}^{(2)}$ with respect to its lower right element (MM), and define $\boldsymbol{\kappa} = (s_2\mathcal{N}^2 2l_M^2 d_M)^{-1}\mathbf{E}^{(2)}$. In the WCL, $\boldsymbol{\kappa} \to \bar{\boldsymbol{\kappa}}$, we then get

$$\bar{\boldsymbol{\kappa}} = \begin{bmatrix} \bar{\mathcal{M}}_B^2\tilde{P}_B^2\tilde{d}_B & \bar{\mathcal{M}}_B\tilde{P}_B\bar{\mathcal{M}}_S\tilde{P}_S\frac{1}{2}(\tilde{d}_B+\tilde{d}_S) & \bar{\mathcal{M}}_B\tilde{P}_B\frac{1}{2}(1+\tilde{d}_B) \\ \bar{\mathcal{M}}_B\tilde{P}_B\bar{\mathcal{M}}_S\tilde{P}_S\frac{1}{2}(\tilde{d}_B+\tilde{d}_S) & \bar{\mathcal{M}}_S^2\tilde{P}_S^2\tilde{d}_S & \bar{\mathcal{M}}_S\tilde{P}_S\frac{1}{2}(1+\tilde{d}_S) \\ \bar{\mathcal{M}}_B\tilde{P}_B\frac{1}{2}(1+\tilde{d}_B) & \bar{\mathcal{M}}_S\tilde{P}_S\frac{1}{2}(1+\tilde{d}_S) & 1 \end{bmatrix}. \tag{15}$$

Note that there is no $\mathcal{N}$-dependence in $\bar{\boldsymbol{\kappa}}$.

Next we consider the matrix elements of $W^{(2)}_{\tau,\tau'}$, which are defined as [10]

$$W^{(2)}_{\tau,\tau'} = \frac{1}{\mathcal{M}_\tau\mathcal{M}_{\tau'}\mathcal{N}^2}\sum_{m\in\tau}\sum_{k\in\tau'}W^{(2)}_{m,k} = \frac{1}{\mathcal{M}_\tau\mathcal{M}_{\tau'}\mathcal{N}^2}\sum_{m\in\tau}\sum_{k\in\tau'}\left(\prod_{(j,j')\in\mathcal{P}_{k,m}}\frac{w^{(2)}_{j,j'}}{w^{(0)}_{j,j'}}\right). \tag{16}$$

Here the product is over all pairs of nearest neighbour segments (j, j') between segments k and m, i.e. the path $\mathcal{P}_{k,m}$ along the chain. The coefficients $w^{(n)}_{j,j'} = w^{(n)}_{\tau,\tau'}$ are nth Legendre

coefficients of $w_{\tau,\tau'}(\hat{\omega}\cdot\hat{\omega}')$ with $j\in\tau$ and $j'\in\tau'$. However, the matrix elements $W^{(2)}_{\tau,\tau'}$ vanish in the case of infinitely long polymers, so therefore we define $\boldsymbol{\alpha}=\mathcal{N}\mathbf{W}^{(2)}$. Furthermore, for notational purposes we also define

$$\sigma_{\tau,\tau'}=w^{(2)}_{\tau,\tau'}/w^{(0)}_{\tau,\tau'}. \tag{17}$$

Here we only show the calculation of the SM element of $\boldsymbol{\alpha}$; the procedure is similar for the remaining elements. From equation (16) we obtain

$$\alpha_{\mathrm{S,M}}=\frac{\mathcal{N}}{\mathcal{M}_{\mathrm{S}}\mathcal{N}^2}\left(\mathcal{N}\sum_{k=1}^{\mathcal{M}_{\mathrm{S}}}\sigma_{\mathrm{S,S}}^{\mathcal{M}_{\mathrm{S}}-k}\sigma_{\mathrm{S,M}}+\sum_{\substack{n,n'=1\\ n\neq n'}}^{\mathcal{N}}\sum_{k=1}^{\mathcal{M}_{\mathrm{S}}}\sigma_{\mathrm{S,S}}^{k-1}\sigma_{\mathrm{B,S}}\sigma_{\mathrm{B,B}}^{|n-n'|\mathcal{M}_{\mathrm{B}}}\sigma_{\mathrm{B,S}}\sigma_{\mathrm{S,S}}^{\mathcal{M}_{\mathrm{S}}-1}\sigma_{\mathrm{S,M}}\right). \tag{18}$$

The contributions to $\alpha_{\mathrm{S,M}}$ come from two distinct sources: the first are contributions from spacer segments k and the mesogen within the same side-chain, $\sigma_{\mathrm{S,S}}^{\mathcal{M}_{\mathrm{S}}-k}\sigma_{\mathrm{S,M}}$. The second contributions are due to mesogens on other side-chains, and consequently are passed on via part of the backbone, $\sigma_{\mathrm{S,S}}^{k-1}\sigma_{\mathrm{B,S}}\sigma_{\mathrm{B,B}}^{|n-n'|\mathcal{M}_{\mathrm{B}}}\sigma_{\mathrm{B,S}}\sigma_{\mathrm{S,S}}^{\mathcal{M}_{\mathrm{S}}-1}\sigma_{\mathrm{S,M}}$. The indices n,n' are used to sum over units, and the indices k,k' are used to sum over segments within a unit. At this point, we note that the sums above can be performed analytically. However, we are interested in the WCL and IBL, so we proceed to these limits directly. The $\sigma_{\tau_p,\tau_{p'}}$ s we need become in the WCL (to first order in βJ_τ)

$$\begin{aligned}
&\sigma_{\mathrm{B,B}}=\frac{\int_{-1}^{1}\mathrm{d}x\,P_2(x)\exp[\beta J_{\mathrm{B}}x]}{\int_{-1}^{1}\mathrm{d}x\exp[\beta J_{\mathrm{B}}x]}\to 1-3\,(\beta J_{\mathrm{B}})^{-1},\\
&\sigma_{\mathrm{S,S}}\to 1-3\,(\beta J_{\mathrm{S}})^{-1},\\
&\sigma_{\mathrm{B,S}}=\int_{-1}^{1}\mathrm{d}x\,P_2(x)\delta(x)=-\tfrac{1}{2},\\
&\sigma_{\mathrm{S,M}}=\sigma_{\mathrm{S,S}}.
\end{aligned} \tag{19}$$

We note that $\sigma_{\mathrm{B,S}}$ is the single element with a negative value and it is this element which forces the oblate backbone conformations. Next, a power of $\sigma_{\tau,\tau}$ ($\tau\in\{B,S\}$) becomes in the WCL

$$\sigma_{\tau,\tau}^{\mathcal{M}_\tau}=\left(1-3\,(\beta J_\tau)^{-1}\right)^{\beta J_\tau\bar{\mathcal{M}}_\tau}\to\exp\left[-3\bar{\mathcal{M}}_\tau\right], \tag{20}$$

where we have used $\lim_{n\to\infty}(1+\frac{x}{n})^n=\exp[x]$. Furthermore, as the backbone and the spacers are continuous, the summations over k and k' (N.B. not the summations over n and n') have to be replaced by integrations. For example, the following sum becomes, using $\bar{k}_{\mathrm{S}}=k/\beta J_{\mathrm{S}}$,

$$\frac{1}{\mathcal{M}_{\mathrm{S}}}\sum_{k=1}^{\mathcal{M}_{\mathrm{S}}}\sigma_{\mathrm{S,S}}^{k}\to\frac{1}{\bar{\mathcal{M}}_{\mathrm{S}}}\int_0^{\bar{\mathcal{M}}_{\mathrm{S}}}\mathrm{d}\bar{k}_{\mathrm{S}}\mathrm{e}^{-3\bar{k}_{\mathrm{S}}}=\frac{1-\mathrm{e}^{-3\bar{\mathcal{M}}_{\mathrm{S}}}}{3\bar{\mathcal{M}}_{\mathrm{S}}}. \tag{21}$$

The summation over n and n' becomes

$$\lim_{\mathcal{N}\to\infty}\frac{1}{\mathcal{N}}\sum_{\substack{n,n'=1\\ n\neq n'}}^{\mathcal{N}}\sigma_{\mathrm{B,B}}^{\mathcal{M}_{\mathrm{B}}|n-n'|}\to\lim_{\mathcal{N}\to\infty}\frac{1}{\mathcal{N}}\sum_{\substack{n,n'=1\\ n\neq n'}}^{\mathcal{N}}\mathrm{e}^{-3\bar{\mathcal{M}}_{\mathrm{B}}|n-n'|}=\frac{2\mathrm{e}^{-3\bar{\mathcal{M}}_{\mathrm{B}}}}{1-\mathrm{e}^{-3\bar{\mathcal{M}}_{\mathrm{B}}}}. \tag{22}$$

Combining these results, we obtain a fairly simple expression for $\bar{\alpha}_{\mathrm{S,M}}$ (in the IBL as well as the WCL, $\boldsymbol{\alpha}\to\bar{\boldsymbol{\alpha}}$),

$$\bar{\alpha}_{\mathrm{S,M}}=\frac{1-\mathrm{e}^{-3\bar{\mathcal{M}}_{\mathrm{S}}}}{3\bar{\mathcal{M}}_{\mathrm{S}}}\left(1+\frac{1}{2}\mathrm{e}^{-3\bar{\mathcal{M}}_{\mathrm{S}}}\frac{\mathrm{e}^{-3\bar{\mathcal{M}}_{\mathrm{B}}}}{1-\mathrm{e}^{-3\bar{\mathcal{M}}_{\mathrm{B}}}}\right). \tag{23}$$

The other elements are similarly calculated,

$$\bar{\alpha}_{\mathrm{B,B}} = \frac{2}{3\bar{\mathcal{M}}_{\mathrm{B}}}, \tag{24}$$

$$\bar{\alpha}_{\mathrm{B,S}} = -\frac{1}{3\bar{\mathcal{M}}_{\mathrm{B}}}\left(\frac{1-\mathrm{e}^{-3\bar{\mathcal{M}}_{\mathrm{S}}}}{3\bar{\mathcal{M}}_{\mathrm{S}}}\right), \tag{25}$$

$$\bar{\alpha}_{\mathrm{B,M}} = -\frac{\mathrm{e}^{-3\bar{\mathcal{M}}_{\mathrm{S}}}}{3\bar{\mathcal{M}}_{\mathrm{B}}}, \tag{26}$$

$$\bar{\alpha}_{\mathrm{S,S}} = \frac{2}{3\bar{\mathcal{M}}_{\mathrm{S}}}\left(1-\frac{1-\mathrm{e}^{-3\bar{\mathcal{M}}_{\mathrm{S}}}}{3\bar{\mathcal{M}}_{\mathrm{S}}}\right)+\frac{1}{2}\left(\frac{1-\mathrm{e}^{-3\bar{\mathcal{M}}_{\mathrm{S}}}}{3\bar{\mathcal{M}}_{\mathrm{S}}}\right)^2\frac{\mathrm{e}^{-3\bar{\mathcal{M}}_{\mathrm{B}}}}{1-\mathrm{e}^{-3\bar{\mathcal{M}}_{\mathrm{B}}}}, \tag{27}$$

$$\bar{\alpha}_{\mathrm{M,M}} = 1+\frac{1}{2}\mathrm{e}^{-6\bar{\mathcal{M}}_{\mathrm{S}}}\frac{\mathrm{e}^{-3\bar{\mathcal{M}}_{\mathrm{B}}}}{1-\mathrm{e}^{-3\bar{\mathcal{M}}_{\mathrm{B}}}}, \tag{28}$$

with $\bar{\boldsymbol{\alpha}}$ symmetrical. We note that the components which are perpendicularly coupled, i.e. BM and SM, have a minus sign in the corresponding element of $\bar{\boldsymbol{\alpha}}$. This is due to the minus sign in $\sigma_{\mathrm{B,S}}$ in equation (19).

In terms of the new matrices $\bar{\boldsymbol{\alpha}}$ and $\bar{\boldsymbol{\kappa}}$ and in the WCL and IBL, the eigenvalue equation becomes

$$\mathbf{c} = -\frac{\eta s_2}{4\pi}\bar{\boldsymbol{\alpha}}\bar{\boldsymbol{\kappa}}\mathbf{c}. \tag{29}$$

This is a 3×3-matrix eigenvalue problem and therefore soluble. The eigenvalues λ of the combined matrix $\bar{\boldsymbol{\alpha}}\bar{\boldsymbol{\kappa}}$ each correspond to a density. The lowest density we identify as the bifurcation density η_* where the nematic solution appears, so

$$\eta_* = -\frac{4\pi}{s_2\max\lambda} = \frac{32}{\pi\max\lambda}. \tag{30}$$

In fact, it is easy to check that $\det(\bar{\boldsymbol{\kappa}}) = 0$, so there are only two nonzero eigenvalues. The corresponding eigenvector $\mathbf{c}_*$ yields the relative degree of order at the bifurcation. Normalizing $\mathbf{c}_*$ such that its third element (M) equals one, $c_{\mathrm{M},*} = 1$, the first two elements are at bifurcation equal to the average order of the backbone and the spacers in units of that of the mesogens.

In I, we showed that we can also calculate the order profile along a polymer, i.e. $c'_{\mathrm{B},*}(\bar{m}_{\mathrm{B}})$ is the relative order along the backbone and $c'_{\mathrm{S},*}(\bar{m}_{\mathrm{S}})$ along the spacer. In the present case of LC polymers in the WCL and the IBL we obtain

$$\mathbf{c}'_*(\bar{m}_{\mathrm{B}},\bar{m}_{\mathrm{S}}) = \begin{pmatrix} c'_{\mathrm{B},*}(\bar{m}_{\mathrm{B}}) \\ c'_{\mathrm{S},*}(\bar{m}_{\mathrm{S}}) \\ 1 \end{pmatrix} = -\frac{\eta_* s_2}{4\pi}\bar{\boldsymbol{\alpha}}'(\bar{m}_{\mathrm{B}},\bar{m}_{\mathrm{S}})\bar{\boldsymbol{\kappa}}\mathbf{c}_*. \tag{31}$$

So after having solved the bifurcation equation (29) one can obtain the order profile via equation (31) by using the bifurcation density η_* and the order vector $\mathbf{c}_*$ *as an input*. The only additional ingredient we need is the new matrix $\bar{\boldsymbol{\alpha}}'(\bar{m}_{\mathrm{B}},\bar{m}_{\mathrm{S}})$, whose elements are calculated in the same way as $\bar{\boldsymbol{\alpha}}$ and are given in the appendix (for more details, we again refer to I). The matrices $\bar{\boldsymbol{\alpha}}$ and $\bar{\boldsymbol{\alpha}}'$ are related through

$$\bar{\boldsymbol{\alpha}} = \frac{1}{\bar{\mathcal{M}}_{\mathrm{B}}\bar{\mathcal{M}}_{\mathrm{S}}}\int_0^{\bar{\mathcal{M}}_{\mathrm{B}}}\mathrm{d}\bar{m}_{\mathrm{B}}\int_0^{\bar{\mathcal{M}}_{\mathrm{S}}}\mathrm{d}\bar{m}_{\mathrm{S}}\,\bar{\boldsymbol{\alpha}}'(\bar{m}_{\mathrm{B}},\bar{m}_{\mathrm{S}}). \tag{32}$$

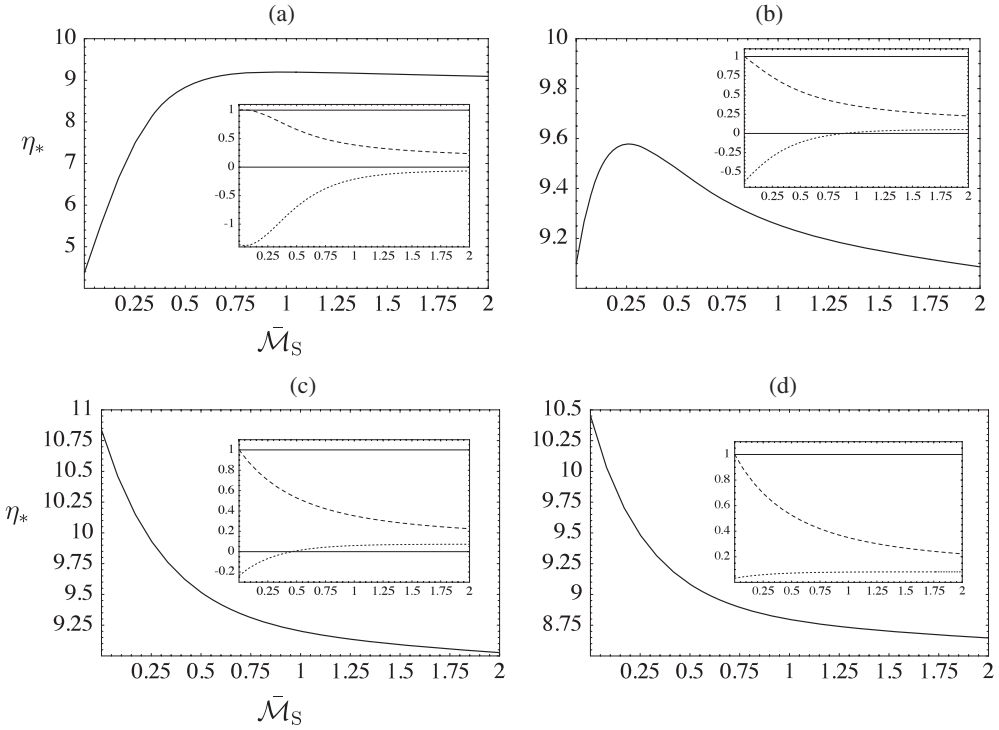

Figure 2. The I–N bifurcation density and the relative order of the components (inset) as a function of spacer length, $\bar{\mathcal{M}}_S$, for various values of the spacer separation, $\bar{\mathcal{M}}_B$. The parameters are $\tilde{d}_B = \tilde{d}_S = 0$, $\tilde{P}_B = \tilde{P}_S = 0.3$ and (a) $\bar{\mathcal{M}}_B = 0.1$, (b) $\bar{\mathcal{M}}_B = 0.4$, (c) $\bar{\mathcal{M}}_B = 1$ and (d) $\bar{\mathcal{M}}_B = 5$. The order of the backbone ($c_{B,*}$, dotted line) and the spacers ($c_{S,*}$, dashed line) is measured in terms of that of the mesogens ($c_{M,*}$, solid line), which is set equal to unity everywhere. For comparison, the bifurcation density of a gas of free mesogens is $32/\pi \approx 10.186$.

3.2. Results

In figures 2(a)–(d), we have plotted the I–N bifurcation density, η_*, and the components of the bifurcating eigenvector, $\mathbf{c}_*$, (inset) as a function of the spacer length $\bar{\mathcal{M}}_S$. The four figures correspond to an increasing spacer separation, $\bar{\mathcal{M}}_B = \{0.1, 0.4, 1.0, 5\}$. The parameter values are not representative of real systems but chosen to exhibit the amount of variation possible.

In figure 2(a), the length of the backbone between side-chains is very small. When in addition the effective spacer length $\bar{\mathcal{M}}_S$ is also small, each mesogen is strongly coupled to the neighbouring mesogens (which are 'closely connected' through spacer and backbone). The I–N transition will therefore be at low densities, due to the relatively rigid nature of the molecule. Upon increasing the spacer length, the mesogens become more decoupled and the transition is postponed to higher densities. Above a certain spacer length, the mesogens are effectively decoupled, and increasing the spacer length further just increases the overall length of the molecule. This results in a decrease of the I–N bifurcation density after passing through a maximum (this effect is better visible in figure 2(b)). For larger backbone lengths, $\bar{\mathcal{M}}_B$, the mesogens are already disconnected for $\bar{\mathcal{M}}_S = 0$ and the $\bar{\mathcal{M}}_S$-dependence of η_* is monotonically decreasing (figures 2 (c) and (d)).

The $\bar{\mathcal{M}}_S$-dependences of the components of $\mathbf{c}_*$ is roughly the same for all four cases, figures 2(a)–(d). The normalization is such that $c_{M,*} = 1$ for all parameters. For small $\bar{\mathcal{M}}_S$, the

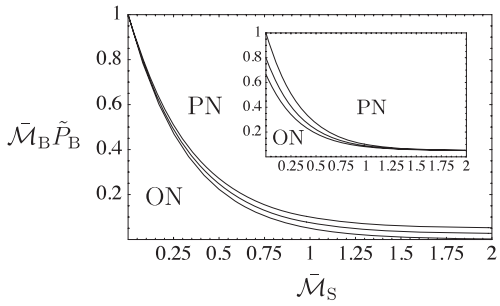

Figure 3. Phase diagram. Combinations of $\bar{\mathcal{M}}_B$ and $\bar{\mathcal{M}}_S$ for which the system has zero backbone order at bifurcation. Parameters are $\tilde{d}_B = \tilde{d}_S = 0$, $\tilde{P}_B = 0.3$ and $\tilde{P}_S = 0.3$ (upper curve), $\tilde{P}_S = 0.15$ (middle curve) and $\tilde{P}_S = 0$ (lower curve). (Inset: parameters are $\tilde{P}_B = \tilde{P}_S = 0.3$, $\tilde{d}_B = \tilde{d}_S = 0$ (upper curve), $\tilde{d}_B = \tilde{d}_S = 0.25$ (middle curve) and $\tilde{d}_B = \tilde{d}_S = 0.5$ (lower curve).) The lower curve in the main figure is the analytical result, equation (34), $\bar{\mathcal{M}}_B\tilde{P}_B = e^{-3\bar{\mathcal{M}}_S}$, and the others are obtained by numerically finding the root of equation (33). For each curve, the system has negative backbone order at bifurcation when its model parameters are below it, and positive when above. If $\bar{\mathcal{M}}_B\tilde{P}_B > 1$ the nematic is always PN.

degree of order of the spacers is close to that of the mesogens, because of their tight coupling. The degree of order of the backbone, however, is very low (often negative even, corresponding to a ON arrangement), because the coupling with the mesogen is strong and perpendicular in orientation. Increasing the spacer length decouples the backbone from the mesogens, and its segments are able to align themselves more with respect to the (infinitesimal) effective molecular field. This means that $c_{B,*}$ increases and it passes through zero at some $\bar{\mathcal{M}}_S$, if it was negative. For the spacers, on average the coupling to the mesogens decreases, causing the average spacer order to go down.

The combination of model parameters, for which the backbone has zero average order at the bifurcation, can be found from

$$c_{B,*} = 0. \tag{33}$$

To analytically solve this equation (containing all six parameters) is impossible as it has a fairly complex transcendental structure, i.e. it is a combination of $e^{-3\bar{\mathcal{M}}_S}$, $\bar{\mathcal{M}}_S$ and powers of them (the same for $\bar{\mathcal{M}}_B$). The cause for this complexity is the dual role that the backbone as well as the spacers play; on the one hand, through the stiffness, they couple orientations on different parts of the chain (yielding factors like $e^{-3\bar{\mathcal{M}}_S}$ and $e^{-3\bar{\mathcal{M}}_B}$), but on the other hand they also contribute to the effective field through their excluded volume interactions (giving factors $\bar{\mathcal{M}}_S$ and $\bar{\mathcal{M}}_B$). It is rather straightforward, however, to construct a numerical scheme to find the roots of equation (33) and the results are presented in figure 3.

We can solve equation (33), analytically, when we put $\tilde{P}_S = 0$. In this way, the spacer has no dimensions (it does not matter what value $\tilde{d}_S$ has) and does not enter into the external field. As $\bar{\mathcal{M}}_S \neq 0$, this means that the mesogens are directly hinged on the backbone with $e^{-3\bar{\mathcal{M}}_S}$ acting as an orientational coupling parameter (large $\bar{\mathcal{M}}_S$, small coupling, and vice versa). If we also set the backbone diameter to zero, $\tilde{d}_B = 0$, we get a very simple relation between the remaining parameters,

$$\bar{\mathcal{M}}_B\tilde{P}_B = e^{-3\bar{\mathcal{M}}_S}. \tag{34}$$

So basically, when the mesogen–backbone coupling, $e^{-3\bar{\mathcal{M}}_S}$, equals the backbone distance between two spacers, the average backbone order at bifurcation is zero (for these polymers without spacers). Moreover, if $\bar{\mathcal{M}}_B\tilde{P}_B > 1$, even for zero spacer length, $\bar{\mathcal{M}}_S = 0$, the nematic is PN (see figure 3).

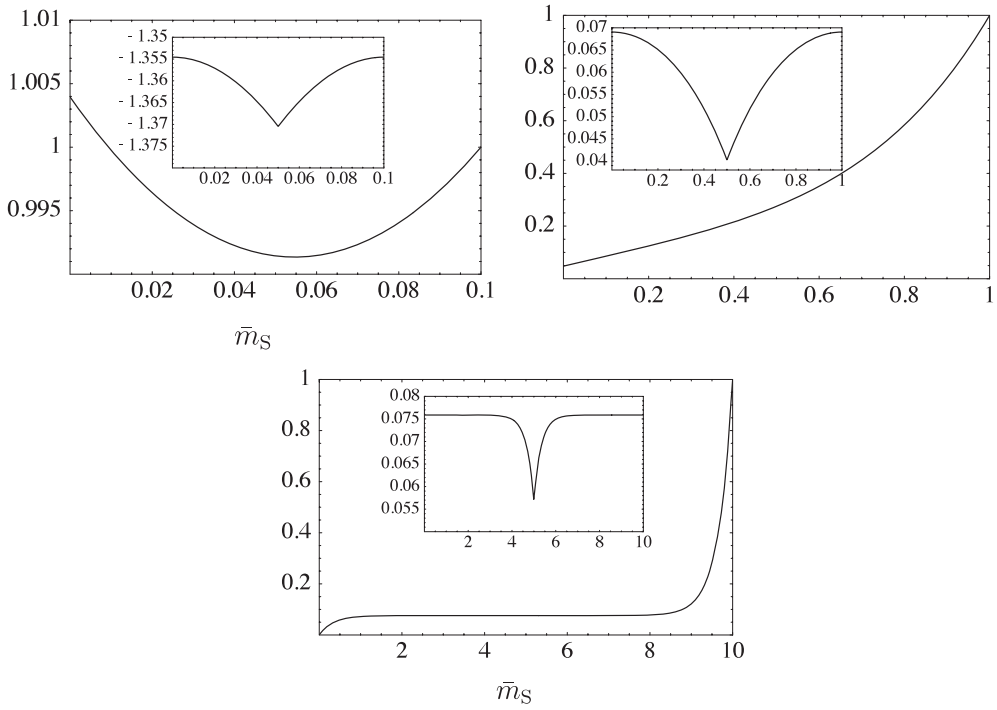

Figure 4. Relative order within the spacers and backbone (inset) at bifurcation. The positions along the backbone are labelled by a continuous parameter running from zero to $\bar{\mathcal{M}}_{\mathrm{B}}$, with the attachment point of the side-chain located at $\frac{1}{2}\bar{\mathcal{M}}_{\mathrm{B}}$. The label of the side-chains runs from zero at the attachment point to the backbone to $\bar{\mathcal{M}}_{\mathrm{S}}$ at the attachment point to the mesogen. The parameters are $\tilde{d}_{\mathrm{B}} = \tilde{d}_{\mathrm{S}} = 0$ and $\tilde{P}_{\mathrm{B}} = \tilde{P}_{\mathrm{S}} = 0.3$. In order to obtain variation in the plots we have varied $\bar{\mathcal{M}}_{\mathrm{B}}$ and $\bar{\mathcal{M}}_{\mathrm{S}}$ simultaneously in each graph; i.e., (top left) $\bar{\mathcal{M}}_{\mathrm{B}} = \bar{\mathcal{M}}_{\mathrm{S}} = 0.1$, (top right) $\bar{\mathcal{M}}_{\mathrm{B}} = \bar{\mathcal{M}}_{\mathrm{S}} = 1$ and $\bar{\mathcal{M}}_{\mathrm{B}} = \bar{\mathcal{M}}_{\mathrm{S}} = 10$ (bottom). The mesogen order is again used as the unit, $c_{\mathrm{M},*} = 1$.

In figure 4, we have plotted the relative degree of order at the bifurcation along the backbone (inset) and spacer for three cases, molecules with very short backbones and spacers, with intermediate lengths and with very long backbones and spacers. Again, the parameter values are chosen to illustrate the possible degree of variation, and do not correspond to realistic cases. The unit of order is again the bifurcating mesogen order, $c_{\mathrm{M},*} = 1$. We first focus on the backbones (inset). If the backbone were completely decoupled from the spacers and mesogens, it would only experience the effective molecular field, and would respond by ordering with respect to it. The case which comes closest to this is when the backbone component is relatively long (figure 4, lower left). In this case, the parts of the backbone in between the spacer hinges hardly experience the effects of the spacers, and therefore order as if they were decoupled. The parts where the spacers are connected are affected and one can see an (exponential) relaxation of the spacer influence on the backbone on moving away from the hinge. For shorter backbones, this relaxation is already less pronounced (figure 4, upper right), and for very short values of $\bar{\mathcal{M}}_{\mathrm{B}}$ (figure 4, upper left) there is basically no relaxation (although the slope is zero halfway between two hinges, but this is due to symmetry). The claim that there is almost no relaxation in the upper left figure of figure 4 is strengthened by the fact that the vertical scale is much smaller than those of the other two figures. From the upper right figure, it is now clear as well that an average zero backbone order does not mean that the whole backbone has zero order, but

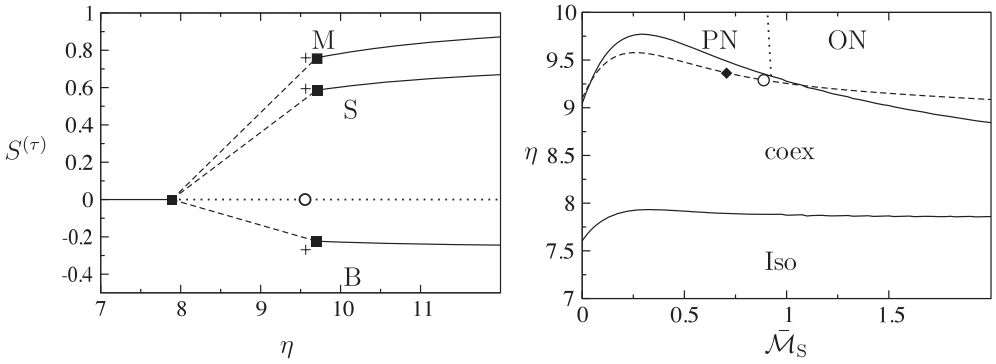

Figure 5. Order as a function of density (left) and phase diagram (right), where both display the I–N coexistence region. The parameters are $\bar{\mathcal{M}}_S = 0.2$ (left) and $\bar{\mathcal{M}}_B = 0.4$, $\tilde{P}_B = \tilde{P}_S = 0.3$, $\tilde{d}_B = \tilde{d}_S = 0$ (left and right). Left: the filled squares are the coexistence (binodal) points and the open circle is the bifurcation (or spinodal) point. The crosses represent the relative order at the bifurcation point, where the degree of order of the mesogen at bifurcation is set equal to the mesogen order at coexistence. Right: the full curves are the coexistence lines, the dashed curve is the bifurcation density and the dotted curve is the ON–PN cross-over, i.e. where $S_B = 0$. The open circle is the bifurcation point where $c_{B,*} = 0$ and the filled diamond is the analytical result of equation (34), $\bar{\mathcal{M}}_S = -\frac{1}{3}\ln(\bar{\mathcal{M}}_B \tilde{P}_B) \approx 0.707$. To compare, the bifurcation density of a gas of free mesogens is $32/\pi \approx 10.186$. The binodal results are generated by the numerical scheme presented in [21].

rather that the negative order of the backbone at the hinges cancels with the positive order of the parts in between the hinges.

Next we consider the spacers. For all three cases, the mesogen is attached at $\bar{m}_S = \bar{\mathcal{M}}_S$ and therefore $c'_{S,*}(\bar{\mathcal{M}}_S) = 1$. The arguments run along the same lines as those for the backbone. Decoupled spacers (both from the backbone and the mesogens) would only experience the external field and would order with respect to this. Again, this is most clear for long spacer lengths (figure 4, lower left). The midpoints of the spacers are effectively decoupled from the backbone and mesogens. The ends are strongly affected, and going towards the middle there is again a (exponential) relaxation. For shorter spacer lengths, the relaxed part of the spacer disappears (figure 4, upper graphs). As a last note, we mention that for the very short backbone and spacers (figure 4, upper left) the relative order of the spacer is even slightly larger than one at the point where it connects to the backbone, $c_{S,*}(0) > c_{M,*}$, although this is a very marginal effect.

Finally, we compare some of the bifurcation results with exact numerical results for the same system presented in [21] in figure 5. On the left in figure 5 we have plotted the order as a function of density close to coexistence. The bifurcation density is located close to the nematic coexistence density, something which we find to occur quite generally. The crosses represent the order at bifurcation where the mesogen order at bifurcation has been equated with the mesogen order at coexistence. The other two crosses give a good indication of the order of the spacers and the backbone. On the right in figure 5 we have given the phase diagram in terms of density versus spacer length $\bar{\mathcal{M}}_S$. The bifurcation density is seen to follow the nematic coexistence density quite closely. The filled circle is the point where the nematic phase bifurcates with zero backbone order. This point is found be close to the point where the dotted curve hits the full curve, which is the actual location of zero backbone order at coexistence. This point is also reasonably estimated by the analytical result of equation (34).

4. Conclusion and discussion

We have studied the isotropic-to-nematic transition in a fluid of side-chain LC polymers. The side-chain LC polymers are explicitly modelled to consist of a (more or less) flexible backbone and lateral spacers and rigid mesogens, thus incorporating the relevant molecular details as well as their branched geometry. Using the segmented chain approach, which we developed in I for very general heteropolymeric systems, we are able to locate the so-called bifurcation density where the nematic solution branches off the isotropic solution. For conceptual simplicity, but also to reduce the number of model parameters, we have applied the wormlike chain limit to the segmented backbone and spacers and we assumed the backbone to be infinitely long. The I–N bifurcation density has been obtained in closed analytical form as a function of the six model parameters. The average backbone order at bifurcation can be negative or positive with respect to that of the mesogens, corresponding respectively to oblate or prolate backbone conformations. We have determined the phase diagram of for which combinations of model parameters an oblate or prolate nematic is formed. Other results include order profiles along the backbone and the spacers. Finally, we have compared some of the bifurcation results with the exact numerical results obtained in [21] for the same system.

In [18, 19], Warner and co-workers (WWR) considered a similar system of polymers consisting of wormlike backbones and laterally hinged rigid mesogen side-groups, but not including spacers as a separate component. Using Maier–Saupe type interactions between the components and the temperature as the thermodynamic variable, they identified three different nematic phases, two of which are the oblate and prolate nematic also considered here, and the third corresponds to a backbone-induced nematic. However, in the WWR-approach, no distinction is made between mesogen–backbone interactions acting through the effective mean field (*inter*chain) or mediated by the connecting hinges (*intra*chain). As a result, the orientational fields of the mesogens act in a delocalized fashion on the backbones and vice versa. In our approach we explicitly distinguish between these two different sources of interaction between the mesogens and the backbone, and include the intrachain (bending) contributions exactly. Consequently, we are able to study the non-uniform order profiles along spacers and backbone due to the connectivity between all the components. Furthermore, the distinction between these two interaction contributions also results in a different scaling: i.e. interchain interactions, which are due to the interaction with other polymers, scale with the density, whereas the intrachain interactions, which are single-polymer effects, are density *in*dependent. The fact that we use a lyotropic (Onsager type) theory where WWR use a thermotropic (Maier–Saupe type) approach is not expected to yield great differences, as the two approaches have an almost identical formal structure. Identifying density with inverse temperature gives a rough correspondence in (phase) behaviour. An additional advantage of the Onsager type interactions over Maier–Saupe interactions is that in this case the dimensions of the molecule totally fix the relative magnitude of the various interactions, whereas these interactions in the WWR approach can be tuned to arbitrary relative magnitudes, which does not necessarily reflect realistic physical behaviour. Our theory does need six model parameters, in contrast to WWR, who use four. This difference is due to the fact that we explicitly take into account the lateral spacer chains, whose dimensions yield two extra model parameters: $\tilde{P}_S$ and $\tilde{d}_S$. In [21] we have already compared the full nematic phase behaviour for the present system to WRR. The most striking difference is that nematic–nematic phase transitions of the type found by WRR are ruled out by a convexity argument on the free energy. This difference can be directly traced to the difference in the way the intrachain degrees of freedom are treated.

Experimental systems of side-chain LC polymers commonly show smectic phases [3, 6, 2, 27, 28]. Indeed, the system we consider, for which we here have calculated the stability

with respect to nematic perturbations, may in principle become unstable with respect to the smectic phase even before becoming a nematic. It would thus be very interesting to include this type of ordering in the present approach and study the competition between smectics and nematics. However, this poses a major theoretical challenge. The bifurcation analysis certainly will become a lot more complicated, as the smectic density would cause non-trivial position–orientation couplings along the polymer. The resulting eigenfunctions of the interaction kernel would no longer follow from a symmetry related argument, as the Legendre polynomials do in the nematic case, but would have to be computed numerically. A first attempt in this direction, which considers the formation lamellar phases in liquid-crystalline heteropolymers, is found in [29]. Polydispersity in the degree of polymerization is also inevitable in experimental systems, but its effect on the I–N phase behaviour is expected to be marginal, justifying our use of infinitely long backbones. In inhomogeneous phases, however, correlations travel much further along the polymers and polydispersity is seen to affect the phase behaviour [2, 28]. Finally, odd–even effects of the transition temperatures are often reported, where e.g. the clearing temperature shows oscillations as a function of spacer length. These could in principle be studied with the present model, but more sophisticated interactions along the chain would be necessary, i.e. between next-nearest-neighbouring segments, modelling e.g. the different rotation-isomeric states that occur in $-(CH_2)-$ chains.

Acknowledgments

This work is part of the research programme of the Stichting voor Fundamenteel Onderzoek der Materie (FOM), which is financially supported by the Nederlandse organisatie voor Wetenschappelijk Onderzoek (NWO).

Appendix. The elements of $\bar{\boldsymbol{\alpha}}'$

In this appendix we give the elements of the matrix $\bar{\boldsymbol{\alpha}}'(\bar{m}_{\rm B}, \bar{m}_{\rm S})$, which is needed to calculate order profiles along the spacers and backbone (equation (31)):

$$\bar{\alpha}'_{\rm B,B} = \bar{\alpha}_{\rm B,B}, \tag{A.1}$$

$$\bar{\alpha}'_{\rm B,S}(\bar{m}_{\rm B}) = -\frac{1}{2}\left(\frac{1-{\rm e}^{-3\bar{\mathcal{M}}_{\rm S}}}{3\bar{\mathcal{M}}_{\rm S}}\right)\left\{{\rm e}^{-3|\bar{m}_{\rm B}-\frac{1}{2}\bar{\mathcal{M}}_{\rm B}|} + \left({\rm e}^{3(\bar{m}_{\rm B}-\frac{1}{2}\bar{\mathcal{M}}_{\rm B})}+{\rm e}^{-3(\bar{m}_{\rm B}-\frac{1}{2}\bar{\mathcal{M}}_{\rm B})}\right)\frac{{\rm e}^{-3\bar{\mathcal{M}}_{\rm B}}}{1-{\rm e}^{-3\bar{\mathcal{M}}_{\rm B}}}\right\}, \tag{A.2}$$

$$\bar{\alpha}'_{\rm B,M}(\bar{m}_{\rm B}) = -\frac{1}{2}{\rm e}^{-3\bar{\mathcal{M}}_{\rm B}}\left\{{\rm e}^{-3|\bar{m}_{\rm B}-\frac{1}{2}\bar{\mathcal{M}}_{\rm B}|} + \left({\rm e}^{3(\bar{m}_{\rm B}-\frac{1}{2}\bar{\mathcal{M}}_{\rm B})}+{\rm e}^{-3(\bar{m}_{\rm B}-\frac{1}{2}\bar{\mathcal{M}}_{\rm B})}\right)\frac{{\rm e}^{-3\bar{\mathcal{M}}_{\rm B}}}{1-{\rm e}^{-3\bar{\mathcal{M}}_{\rm B}}}\right\}, \tag{A.3}$$

$$\bar{\alpha}'_{\rm S,B}(\bar{m}_{\rm S}) = -\frac{1}{3\bar{\mathcal{M}}_{\rm B}}{\rm e}^{-3\bar{m}_{\rm S}}, \tag{A.4}$$

$$\bar{\alpha}'_{\rm S,S}(\bar{m}_{\rm S}) = \frac{1}{3\bar{\mathcal{M}}_{\rm S}}\left(2-{\rm e}^{-3\bar{m}_{\rm S}}-{\rm e}^{-3(\bar{\mathcal{M}}_{\rm S}-\bar{m}_{\rm S})}+\frac{1}{2}{\rm e}^{-3\bar{m}_{\rm S}}\left(1-{\rm e}^{-3\bar{\mathcal{M}}_{\rm S}}\right)\frac{{\rm e}^{-3\bar{\mathcal{M}}_{\rm B}}}{1-{\rm e}^{-3\bar{\mathcal{M}}_{\rm B}}}\right), \tag{A.5}$$

$$\bar{\alpha}'_{\rm S,M}(\bar{m}_{\rm S}) = {\rm e}^{-3(\bar{\mathcal{M}}_{\rm S}-\bar{m}_{\rm S})}+\frac{1}{2}{\rm e}^{-3\bar{\mathcal{M}}_{\rm S}-3\bar{m}_{\rm S}}\frac{{\rm e}^{-3\bar{\mathcal{M}}_{\rm B}}}{1-{\rm e}^{-3\bar{\mathcal{M}}_{\rm B}}}, \tag{A.6}$$

$$\bar{\alpha}'_{\rm M,B} = \bar{\alpha}_{\rm M,B}, \tag{A.7}$$

$$\bar{\alpha}'_{\rm M,S} = \bar{\alpha}_{\rm M,S}, \tag{A.8}$$

$$\bar{\alpha}'_{\rm M,M} = \bar{\alpha}_{\rm M,M}. \tag{A.9}$$

Here, $\bar{m}_{\mathrm{B}} \in [0, \bar{\mathcal{M}}_{\mathrm{B}}]$ where $\bar{m}_{\mathrm{B}} = 0$ and $\bar{m}_{\mathrm{B}} = \bar{\mathcal{M}}_{\mathrm{B}}$ are the same (because the backbone is infinitely periodic) in between the spacers and $\bar{m}_{\mathrm{B}} = \frac{1}{2}\bar{\mathcal{M}}_{\mathrm{B}}$ is where the spacer is attached to the backbone. Further, $\bar{m}_{\mathrm{S}} \in [0, \bar{\mathcal{M}}_{\mathrm{S}}]$ where $\bar{m}_{\mathrm{S}} = 0$ is on the backbone side of the spacer and $\bar{m}_{\mathrm{S}} = \bar{\mathcal{M}}_{\mathrm{S}}$ is on the mesogen side of the spacer. In contrast with $\bar{\boldsymbol{\alpha}}$, $\bar{\boldsymbol{\alpha}}'$ is not symmetric. Obviously, the elements $\bar{\alpha}'_{\mathrm{M},\tau} = \bar{\alpha}_{\mathrm{M},\tau}$ have no $\bar{m}_{\mathrm{M}}$-dependence as there is only one mesogen in a unit. Also $\bar{\alpha}'_{\mathrm{B,B}} = \bar{\alpha}_{\mathrm{B,B}}$ has no $\bar{m}_{\mathrm{B}}$-dependence due to the complete translational symmetry along the infinite backbone.

References

[1] Donald A and Windle A 1992 *Liquid Crystalline Polymers* (Cambridge: Cambridge University Press)
[2] Shibaev V and Lam L (ed) 1994 *Liquid Crystalline and Mesomorphic Polymers* (Berlin: Springer)
[3] McArdle C B (ed) 1989 *Side Chain Liquid Crystalline Polymers* (Glasgow: Blackie)
[4] Ciferri A, Krigbaum W R and Meyer R B (ed) 1982 *Polymer Liquid Crystals* (New York: Academic)
[5] Platé N A and Shibaev V P 1987 *Comb-Shaped Polymers and Liquid Crystals* (New York: Plenum)
[6] Demus D, Goodby J, Gray G W, Spiess H-W and Hill V (ed) 1998 *Handbook of Liquid Crystals* vol 3 *High Molecular Weight Liquid Crystals* (New York: Wiley–VCH)
[7] Finkelmann H, Ringsdorf H and Wendorff J H 1978 *Makromol. Chem.* **179** 273
[8] Finkelmann H, Ringsdorf H, Siol W and Wendorff J H 1978 *Makromol. Chem.* **179** 829
[9] Finkelmann H, Happ M, Portugal M and Ringsdorf H 1978 *Makromol. Chem.* **179** 2541
[10] Wessels P P F and Mulder B M 2006 Isotropic-to-nematic transition in LC heteropolymers: I. Formalism and main chain LC polymers *J. Phys.: Condens. Matter* **18** 9335
[11] Onsager L 1949 *Ann. New York Acad. Sci.* **51** 627
[12] Maier W and Saupe A 1959 *Z. Naturf.* **14** 882
[13] Khokhlov A R and Semenov A N 1981 *Physica* A **108** 546
[14] Khokhlov A R and Semenov A N 1982 *Physica* A **112** 605
[15] Warner M, Gunn J M F and Baumgärtner A B 1985 *J. Phys. A: Math. Gen.* **18** 3007
[16] Semenov A N and Khokhlov A R 1988 *Sov. Phys.—Usp.* **31** 988
[17] Vasilenko S, Shibaev V and Khokhlov A 1985 *Makromol. Chem.* **186** 1951
[18] Wang X and Warner M 1987 *J. Phys. A: Math. Gen.* **20** 713
[19] Renz W and Warner M 1988 *Proc. R. Soc.* A **417** 213
[20] Bladon P, Warner M and Liu H 1992 *Macromolecules* **25** 4329
[21] Wessels P P F and Mulder B M 2003 *Europhys. Lett.* **64** 337
[22] Evans R 1979 *Adv. Phys.* **28** 143–200
[23] Vroege G J and Lekkerkerker H N W 1992 *Rep. Prog. Phys.* **55** 1241
[24] Holyst R and Oswald P 2001 *Macromol. Theory Simul.* **10** 1
[25] Wessels P P F and Mulder B M 2003 *Soft Mater.* **1** 313
[26] Flory P J 1989 *Statistical Mechanics of Chain Molecules* (Munich: Hanser)
[27] Noirez L, Boeffel C and Daoud-Aladine A 1998 *Phys. Rev. Lett.* **80** 1453
[28] Ostrovskii B, Sulyanov S N, Boiko N I, Shibaev V P and de Jeu W H 2001 *Eur. Phys. J.* E **6** 277
[29] Wessels P P F and Mulder B M 2004 *Phys. Rev.* E **70** 031503